

EXPERIMENTAL APPROACH FOR IMPROVING THE MASS FLOW RATE OF AXIAL FLOW COMPRESSORS BY CHANGING THE DIMENSIONS OF THEIR L-SHAPE INLETS

BY

H. HEIKAL*

S.M. ABD EL-LATIF**

ABSTRACT

Experiments to determine the effects of the dimensions of the L-shape entrance of axial flow compressors on different flow parameters, were carried. A test rig was built. Instruments to measure velocities and pressures were designed, constructed and calibrated.

The conclusions obtained are believed to be practically useful in the design of axial flow compressor entrance. There are two main conclusions obtained :

- a. The optimum mass flow rate distribution is obtained when the width to depth ratio of the L-shape inlet is about 2.
- b. The most effective movement of the inlet plates on the mass flow rate distribution is that of the vertical plate movement.

INTRODUCTION

Due to some severe conditions, it becomes impossible to provide the axial flow compressors with ideal inlets, and instead; the L-shape inlets are used. The use of an unsuitable intake affects the compressor performance, and the effects may appear as a decrease in efficiency and an increase in vibrations.

* Professor, Faculty of Engineering and Technology, Mattaria, Helwan University.

** Associate Professor, Faculty of Petroleum and Mining Engineering, Suez canal university.

The present work is a trial to give an answer to the question about the most suitable dimensions of the L-shape inlet which can give the best mass flow distribution near the compressor face.

Experimental approach for tackling this problem was tried. A test rig was constructed and special instruments were made to suit the required specific readings.

The results taken, being numerous, necessitated the use of a computer for processing, and hence a suitable computer program had to be done. The following conclusions have been deduced :

The optimum specific dimensions of the L-shape entrance that gives the desired parameters for the best mass flow distribution has been found to be at the ratio :

$$\text{width/depth} \cong 2$$

Also, it has been deduced that the vertical plate movement has considerable effect on the performance more than the movement of the bottom plate.

LITERATURE REVIEW

It is well known that the efficiencies of the axial flow compressors are low by themselves compared by machines used for the same purpose. Therefore, it becomes a good practice to provide these machines with ideal inlets, but this is not always possible. Some compulsory conditions may necessitate the use of L-shape inlets. Such inlets affect the performance of the axial flow compressors seriously due to some flow problems which may be raised.

A non-uniform velocity distribution at the compressor inlet may cause poor performance, or even cause fatigue failure of compressor blading (1). A standing vortex developed close to the machine intake has been observed using smoke tracing tests. This vortex is believed to be another cause of compressor failure(2).

The ideal inlet shape, giving the best flow pattern can be achieved by theoretical treatment, using the well known laplace equations for potential flow, but the resulting calculations should be checked with model tests. Considerable experience has been gained in this respect, specially in draft tube design, and in the intakes of axial flow pumps (3).

Sometimes, and due to space limitations, the L-shape inlet may be the only one which may suit the existing situation, as it is the case in some marine gas turbines. Theoretical calculations for such a case can not be reliably attained, because of the sharp changes in flow direction and the resulting non-uniformity in the flow.

Experimental treatment in this case may be a simple possible way to attain the conditions leading to the best mass flow distribution.

APPARATUS AND EXPERIMENTAL PROCEDURE

Experimental study becomes necessary to investigate the effects of the inlet shape dimensions on the flow parameters. They are mainly; the velocity, the pressure and the mass flow rate distributions at a suitable section before the compressor face. The determination of the dimensions which specify the optimum inlet shape, would be possible in this case.

For that purpose, a test rig had to be designed and constructed. Also, some instruments might be manufactured to suit the required measurements.

1. THE TEST RIG

A test rig was designed and constructed at the Faculty of Engineering and Technology, Mataria (Helwan University). Fig. (1) shows the details of this test rig which is composed of the following main parts :

a- The L-shape inlet duct

This duct is built in such a way to allow for any change in the inlet dimensions. The farther vertical plate facing the blower is allowed to move back and forth through the range $(X_{\infty} - X_0)$, while the bottom plate is allowed to move up and down through the range $(Z_{\infty} - Z_0)$ as can be seen in Fig. (3).

b- The blower

The blower is of the axial type, and it is driven by a synchronous motor of 7.5 horse power, and a speed of 2900 r.p.m. In place of the blower hub, a wooden shaft of 240 mm diameter and 210 mm long is mounted in order to simulate the actual conditions in practice. On the otherhand an aluminum cone is fixed at the end of the extended shaft to the vertical plate to prevent vortex formation.

The annular entrance to the blower, consists of a wooden horizontal passage of a suitable thickness. Four groups of holes were drilled at the top, bottom, right and left sides of the passage. Each group is composed of five wall tapplings as illustrated in Fig. (4). A butter-fly valve is mounted just after the blower, for the purpose of flow control.

2. MEASURING INSTRUMENTS

Special types of instruments must be prepared to fit our purpose for the specific measurements. These instruments are: the five-hole spherical pitot probe, the multitube inclined manometer, and the vertical manometers.

a- The five-hole spherical pitot-probe

To measure the flow velocity in all directions, a five-hole spherical pitot-probe, with a spherical sensing head of 6 mm diameter, was designed and manufactured at the workshops of the Ministry of Irrigation.

Calibration tests were carried out using a wind tunnel equipped with the necessary calibration requirements. A calibration chart has been prepared according to the detailed informations given by different authors (5) and (6). This chart can be referred to in Appendix B.

b- The manometers

A multi-tube inclined manometer was prepared to be used with the pressure probe. The manometer is composed of 10 tubes with inclination angle 45° .

On the other hand, two vertical U-tube water manometers were arranged to measure the static pressure around the annular entrance, where the wall tapings are spaced 15° apart.

PROGRAM OF EXPERIMENTATION

The following measurements are necessary for the present investigations :

1. The velocity of flow in all directions at a suitable section before the blower.

2. The static pressure variations around the circumference at the selected section.

All these measurements are required at each location of the vertical and bottom plates through the ranges indicated in Fig. (3), with the discharge valve being fully open, which is the case of full-load operation.

THEORETICAL CONSIDERATIONS

For the purpose of the calculations required, some relations must be derived for both velocity and for the mass flow rate.

1- Velocity calculations

At a selected section before the blower face, where the measurements are carried out, we have :

The total pressure at any point in the flow is given by :

$$P_{total} = P_{st} + \frac{1}{2} \rho C^2 \text{ ————— (1) where :}$$

ρ represents the fluid density and C is the free stream velocity (complete nomenclature is given in Appendix A).

On the otherhand, if the energy equation is applied between a point in the free stream and the nth hole on the spherical head of the pressure probe we get :

$$P_{st} + \frac{1}{2} \rho C^2 = P_n + \frac{1}{2} \rho C_n^2 \text{ ————— (2) where :}$$

n indicates the hole number 1, 2, 3, 4 and 5.

solving equations (1) and (2) we have :

$$P_n = P_{st} + \frac{1}{2} \rho C^2 \left\{ 1 - \left(\frac{C_n}{C} \right)^2 \right\} \text{ ————— (3)}$$

putting $\left\{ 1 - \left(\frac{C_n}{C} \right)^2 \right\} = K_n$ and $\frac{1}{2} \rho C^2 = q$ equation (3)

becomes :

$$P_n = P_{st} + K_n q \quad \text{————— (4) where :}$$

K_n is called the pressure recovery factor and it is only a function of the two angles α and δ , which can be referred to in Appendices A and B. Equation (4) can then be arranged to be readily used with the inclined manometer readings, and therefore we can have the following two equations :

$$\begin{aligned} - P_2 \sin \phi + P_B &= P_{st} + K_2 q' \quad) \\ - P_4 \sin \phi + P_B &= P_{st} + K_4 q' \quad) \end{aligned} \quad (5)$$

where: P_B represents the barometer reading, and ϕ is the inclination angle (45°).

subtracting and arranging we get :

$$q' = \frac{(P_4 - P_2)}{(K_2 - K_4)} \sin \phi \quad \text{————— (6)}$$

K_2 and K_4 can be obtained from the calibration chart knowing that the calibration factor k_α is given by the following expression (4) and (5) :

$$K = \frac{(P_2 - P_4)}{(P_3 - P_5)} = f(\alpha) \quad \text{————— (7)}$$

while P_1, P_2, P_3, \dots are the inclined manometer readings through the corresponding holes.

The velocity term C can then be obtained from the calculated value of q' and once the velocity C is known, the various components can be calculated according to the following expressions :

$$\begin{aligned} C_x &= C \cos \alpha \cos \delta . \\ C_y &= C \cos \alpha \sin \delta . \quad \text{————— (8)} \\ C_z &= C \sin \alpha . \end{aligned}$$

One set of measurements, will be given here as an example, while the whole measurements can be referred to in Appendix C.

1. Selected measurements

The following are experimental measurements taken at the vertical plate position $x = 37.5$ cm, and the bottom plate position : $Z = 42$ cm.

Lower half	$x=37.5$ cm, $Z=42$ cm				station 1 temp.atmos. 20°C 757 mm Hg
r mm	P_{15} mm H_2O	P_2 mm H_2O	P_3 mm H_2O	P_4 mm H_2O	δ°
230	-55	-83	-15	-15	+7
220	-62	-91	-21	-17	+5
210	-64	-97	-62	-16	+15
200	-66	-99	-26	-16	+15
190	-67	-100	-28	-15	+15
180	-70	-100	-29	-16	+14
170	-67	-99	-28	-15	+14
160	-67	-97	-27	-15	+17
150	-66	-95	-27	-15	+13
140	-61	-88	-20	-14	+10
130	-57	-81	-20	-15	+8

TABLE (1): Inclined manometer readings at the corresponding dihedral angles.

$P_B = 75.85$ cm Hg	Tem p. : 23°C.					Lower half.		
θ°	0	15	30	45	60	75	90	
P_{st} cm H_2O (Abs)	1027.03	1025.69	1026.39	1026.75	1026.4	1026.25	1025.54	

TABLE (2); Static pressures as measured by the vertical manometer in the lower half.

2. Mass-flow rate calculations

To calculate the mass-flow rate for both the upper half and the lower half of the annular selected section, the mean axial velocity for each half should be computed.

Separate axial velocity profiles are to be plotted for this purpose and then, the mean ordinates can be obtained. Making use of the static pressure measurements around the circumference, the mean density for each half can be computed.

The mass flow rate can then be calculated for each half alone and for all positions of the vertical and bottom plates using the equation :

$$M = \rho A C_m \quad \text{---} \quad (9)$$

Where A represents half the annular area at the selected section.

EXPERIMENTAL RESULTS

Measurements were taken at five stations using the pitot probe to select the most desirable section to be used for carrying out the experimental program. Station (1) shown in Fig. (4) proved to be the best. Measurements were recorded for each position of both the vertical and bottom plates through the ranges indicated in Fig. (3).

A computer program was prepared for calculations, and complete records for the velocities, the static pressures, and the mass flow rates at the selected section were already obtained. It was necessary to concise this bulky body of results, in order to achieve the required inlet dimensions.

DISCUSSION OF RESULTS

The variations in the mean axial velocity difference Δ cm between the upper and the lower halves of the selected section are shown in Fig. (5) for all positions of the vertical and bottom plates x and z , while Fig. (6) gives the relation between the mean axial velocity cm in each half and $\frac{x}{z}$, the dimensionless ratio. Fig. (7) shows the whole relation presented in a dimensionless form, where Δ cm is expressed as a percentage of the average mean axial velocity.

From the previous figures, it can be observed that the best conditions of flow occur when the ratio $\frac{x}{z} = 2.09$, or in other words, when $x=2.156 d$, and $z=1.031 d$, where d is the duct inside diameter before the blower.

Again, it becomes more significant, if the mass flow rates are plotted instead of velocities. The representation in this way will not only indicate the mass flow rate distribution between the upper and the lower halves, but it will give also an indirect indication about the uniformity of the static pressure across the whole section, since the densities computed from the static pressure measurements, are included in mass flow rate calculations. These new relations are shown in Figures (8), (9) and (10). From Fig. (10), the relation between the mass flow rate and the position of the plates, is shown presented in a dimensionless way.

It can be observed at once that the best distribution of the mass flow rate between the two annular halves, occurs at the ratio $\frac{x}{z} = 2.09$, which agrees completely with the results obtained from the velocity representation.

Now, we can say that the minimum deviation of the flow from the ideal conditions, occurs at the previous specified proportions, and away from which the deviations increase.

The above results indicate that the optimum dimensions that give the best distribution are thought to occur where a stabilized cushion at the bottom is created and the local eddies are therefore minimized.

CONCLUSIONS

Two main conclusions, which are believed to be of considerable practical importance; have been deduced.

The first one concerns with the inlet-size dimensions. It indicates that the best flow performance when using L-shape inlet is obtained when the width to depth ratio is about 2.

The second conclusion is dealing with the most effective movement of the inlet plates. It is found that the movement of the vertical plate is more effective.

REFERENCES

- 1] Reid, C. "The Response of Axial Flow Compressors to Intake Flow Distortion" American Society of Mechanical Engineers, Paper 69-Gt-29, 1969.
- 2] Miller, C.L. Sjort Course on : "Small Craft Engineering" 1969, University of Michigan.
- 3] Nechleba, M. "Water Turbines, Their Design and Construction" John Wiley and Sons, London 1965.

- 4] Gouda, W.M.G., "Study of the Inlet Effects on Flow Rate Distribution For Axial Fans" A Master Thesis, Helwan University, 1983.
- 5] Heikal, H. "Three Dimensional Measurements of Aerodynamic Flow by Means of Pressure Probes" 47 Heft 11, Technisches Messen, 1980.
- 6] Lee, J.C., and Ash., J.E. "A Three Dimensional Spherical Pitot-Probe". Trans. ASME. 78 page 603, 1956.

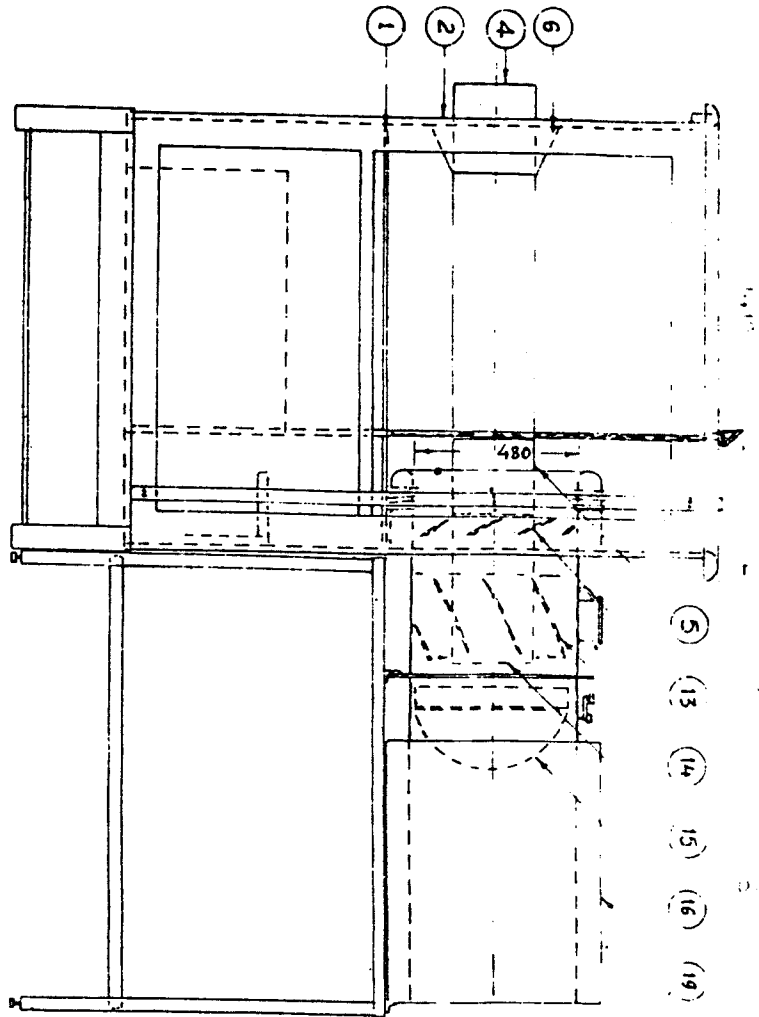
APPENDICES

Appendix A : Nomenclature.

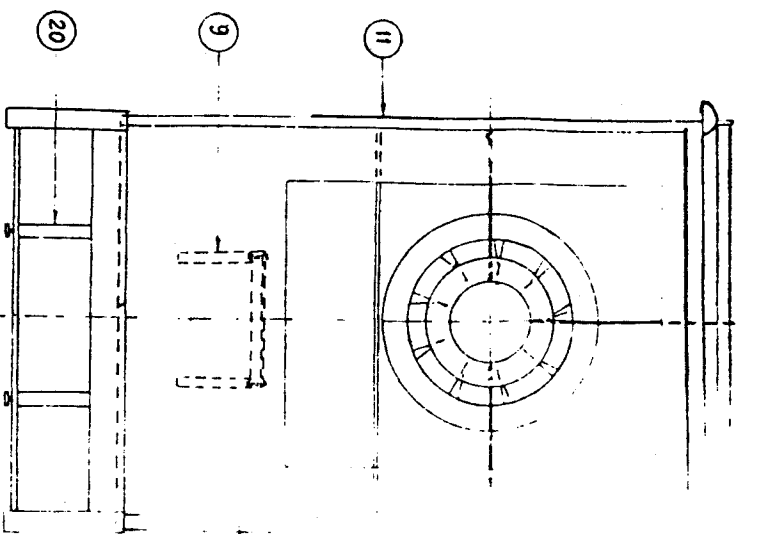
Appendix B : Calibration chart and Computer program.

NOMENCLATURE

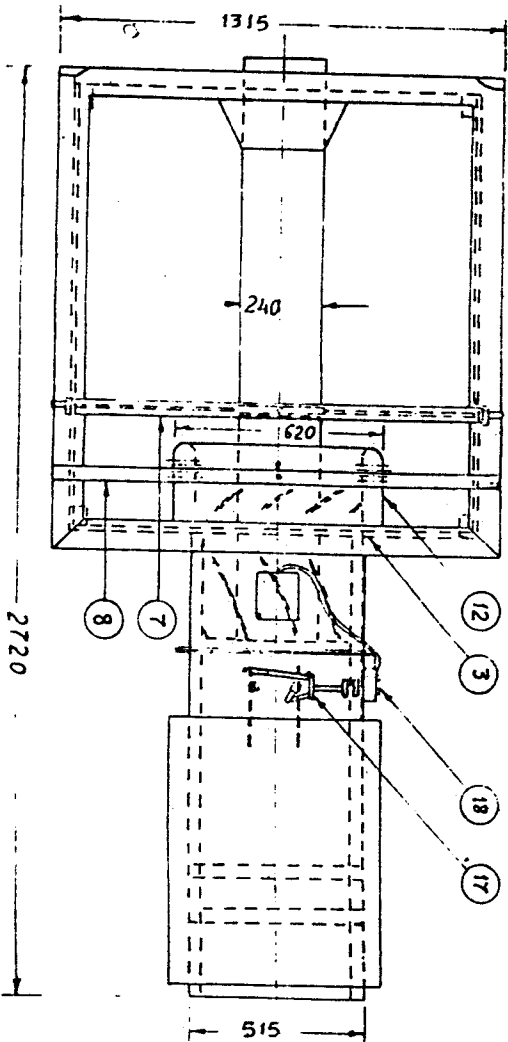
- C : Free stream velocity.
- C_m : Mean axial velocity.
- C_{m1} : Mean axial velocity (lower half).
- C_{mu} : Mean axial velocity (upper half).
- ΔC_m : Difference between upper and lower mean axial velocities.
- C_n : Velocity at the nth hole of the pressure probe.
- C_x : Axial velocity.
- C_y : Velocity in y-direction.
- C_z : Velocity in z-direction.
- d : Inside diameter of the duct before the blower.
- K_n : Pressure recovery factor at the nth hole of the pressure probe.
- K_α : Calibration factor = $\frac{P_2 - P_4}{P_3 - P_{15}}$
- M : Mass flow rate
- M_1 : Mass flow rate in the lower half of the annular entrance.
- M_u : Mass flow rate in the upper half.
- ΔM : Difference between upper and lower mass flow rates.
- P_B : Barometric pressure.
- P_n : Pressure at the nth hole of the pressure probe.
- P_{st} : Static pressure.
- P_{tot} : Total pressure.
- q : Kinetic energy = $\frac{1}{2} \rho C^2$. (q': kinetic energy head $\frac{C^2}{2g}$)
- x : Distance of the vertical plate measured from the blower face.
- Z : Distance of the bottom plate measured from the blower axis.
- α : The angle between the pressure probe axis and it's new position.
- δ : The dihedral angle between the flow plane and the meridian plane.
- ρ : Fluid density.
- ϕ : The angle of inclination of the multi-tube manometer = 45° .



ELEVATION



SIDE VIEW



PLAN

MINIMUM CLEARANCE

NO	DESCRIPTION
20	STAND FOR THE BLOWER
19	SILENCER
18	SWITCH
17	MECHANISM FOR CONTROL THE VALVE
16	BLOWER'S CONTROL VALVE
15	MOTOR
14	STATOR
13	ROTOR
12	CIRCULAR ENTRANCE
11	LEFT SUPPORT FOR P.P
10	RIGHT SUPPORT FOR P.P
9	LOWER SUPPORT FOR P.P
8	UPPER SUPPORT FOR P.P
7	SUPPORT FOR EXTENDED SHAFT
6	ALUMINUM CONE
5	ROTATING SHAFT
4	EXTENDED SHAFT
3	FIXED PLATE
2	VERTICAL PLATE
1	LOWER HORIZONTAL PLATE

COMPONENT PARTS LIST

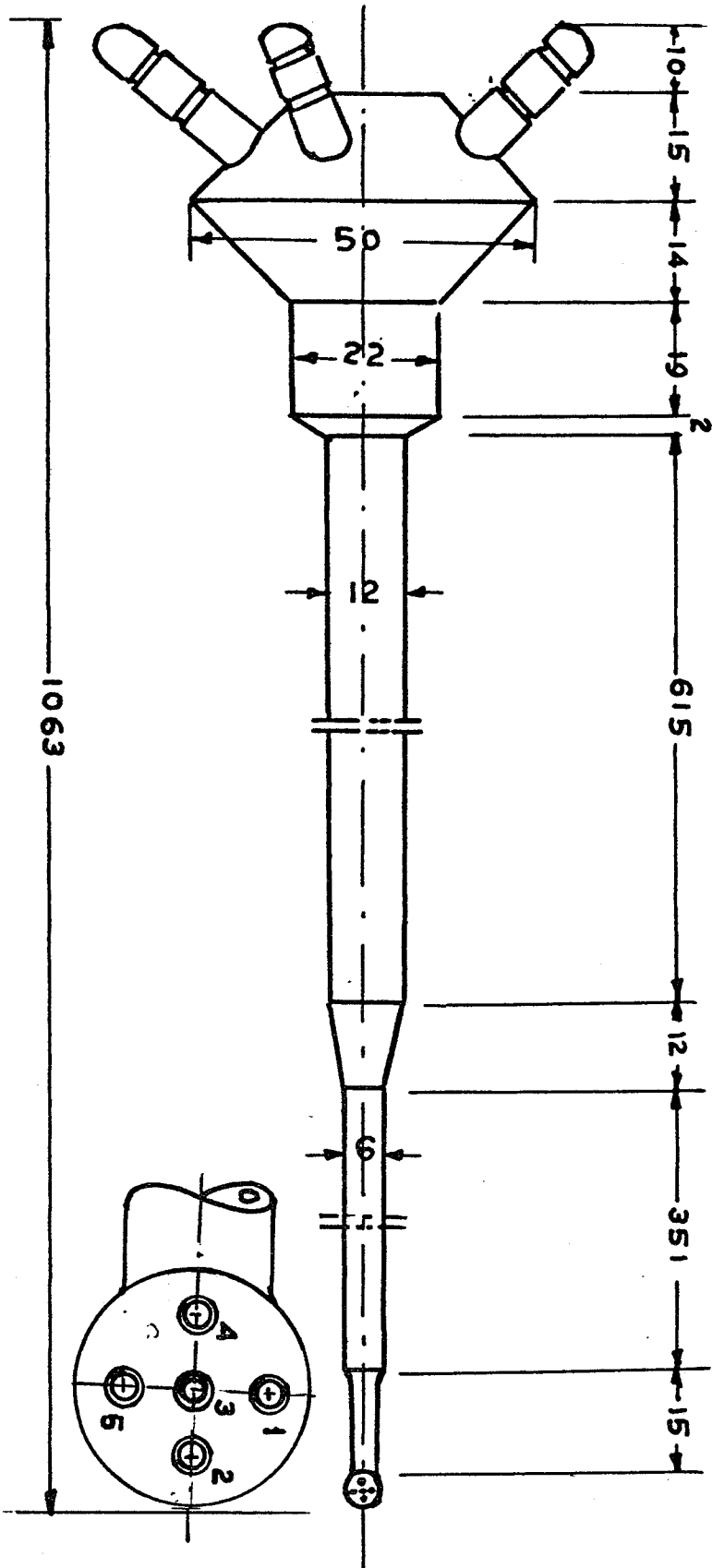


FIG.(2) : FIVE HOLES SPHERICAL PITOT PROBE (DIM.S.IN mms).

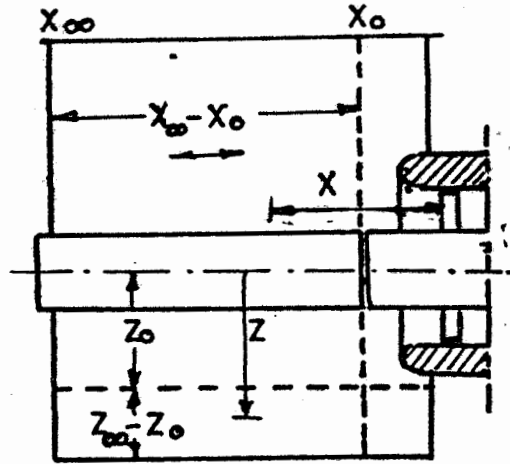


FIG.(3): EXTREME POSITIONS FOR THE VERTICAL AND BOTTOM PLATES

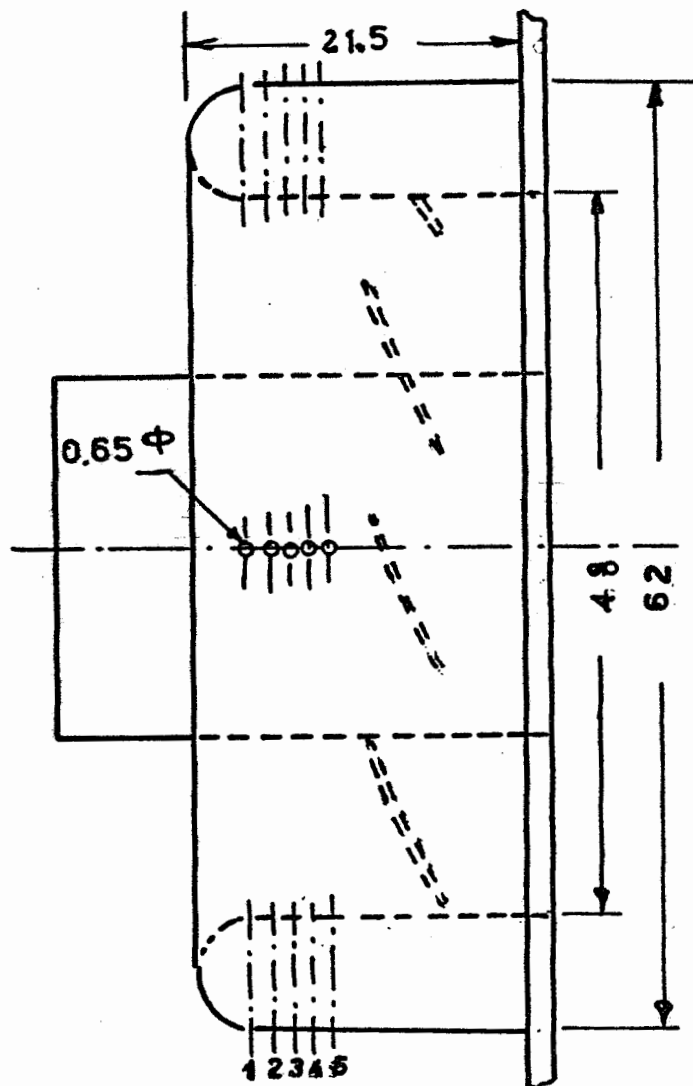


FIG.(4): ANNULAR ENTRANCE AND DISTRIBUTION OF THE FIVE HOLES

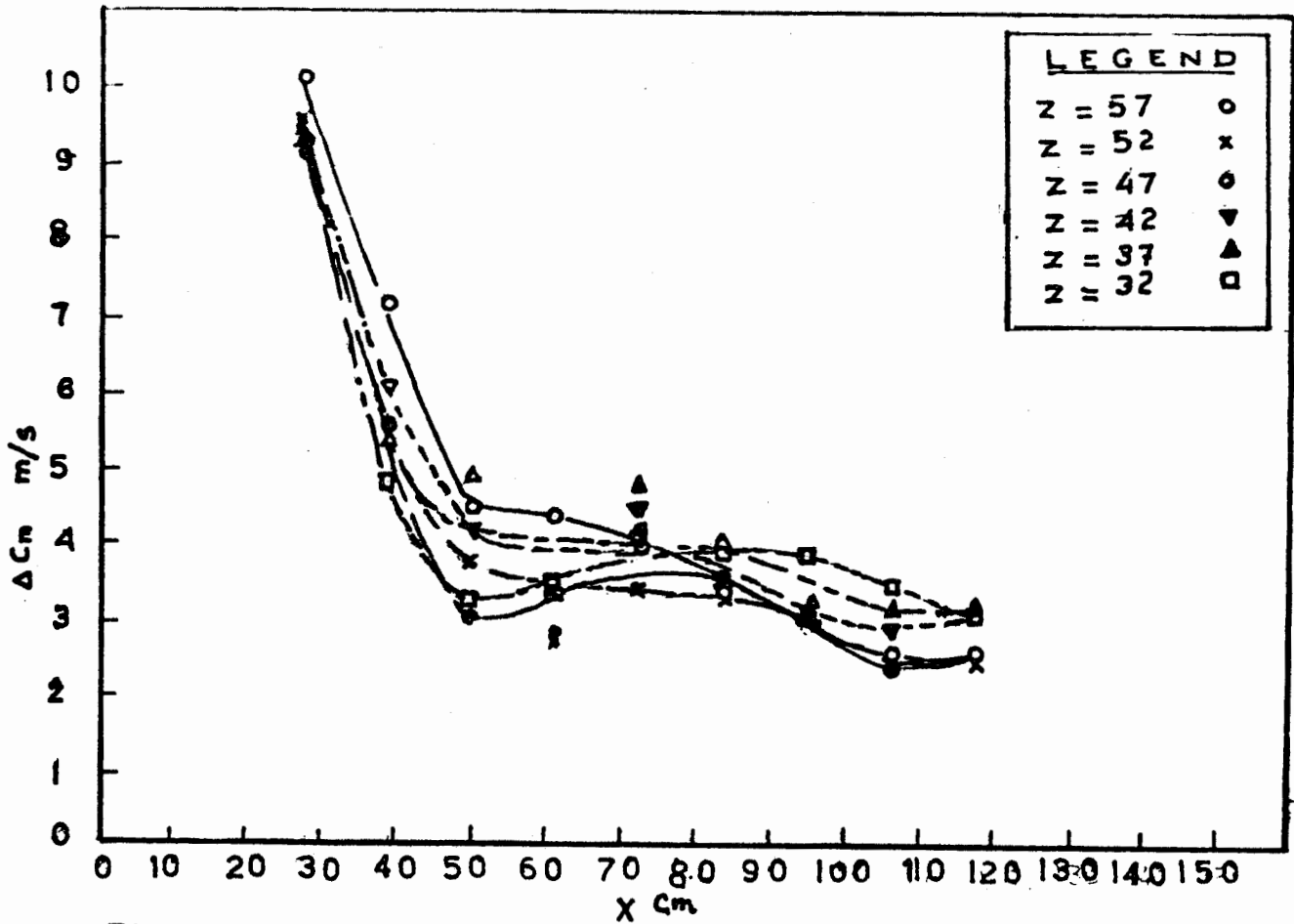


FIG (5): EFFECT OF X AND Z ON THE AXIAL VELOCITY DIFFERENCE

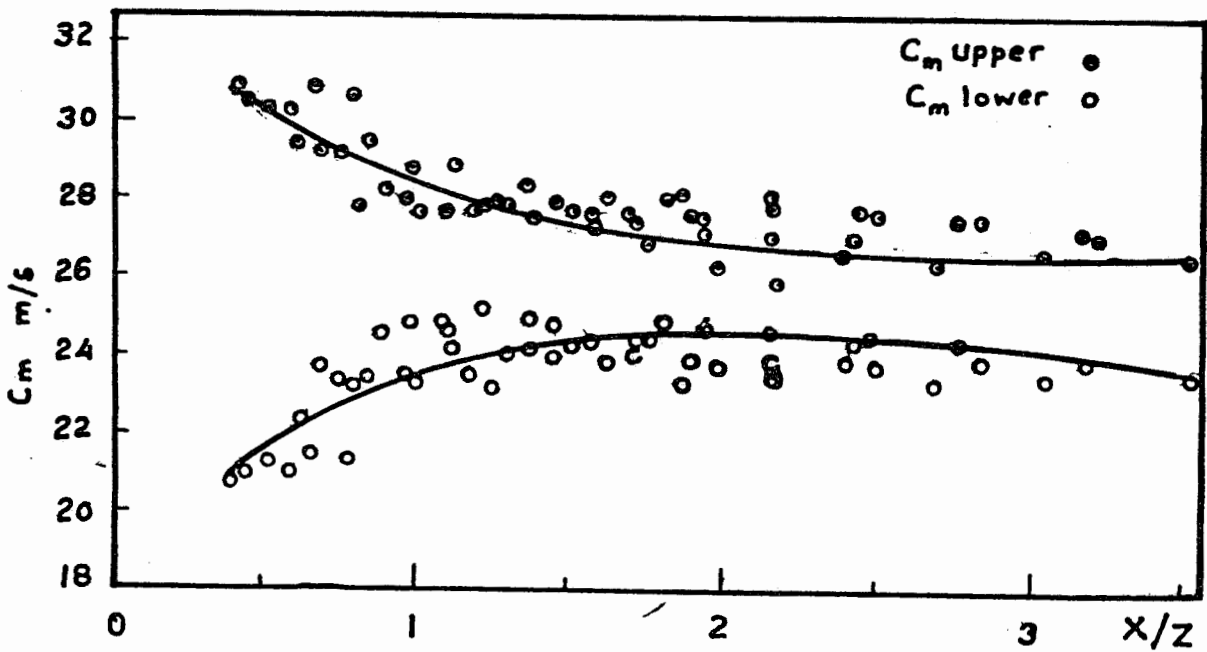


FIG (6): VARIATION IN AXIAL VELOCITY WITH THE RATIO x/z .

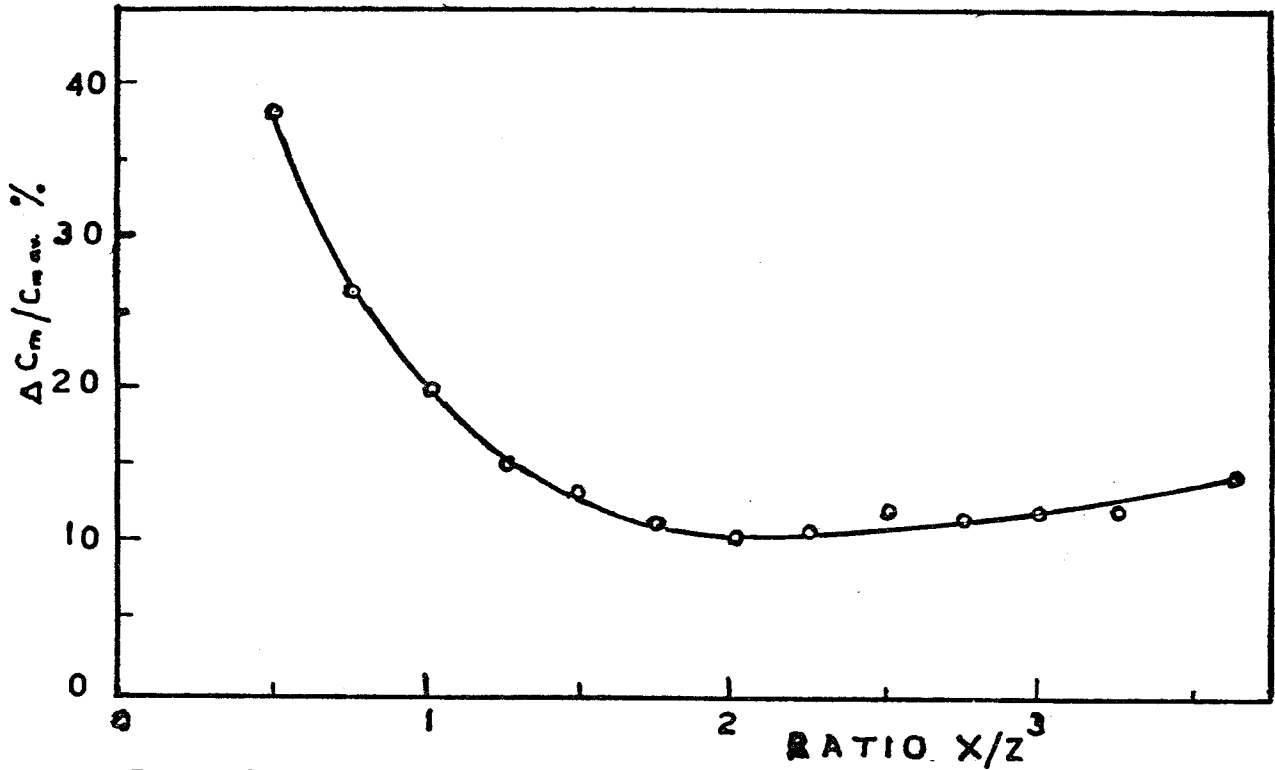


FIG.(7): VARIATION IN PERCENTAGE VEL. DIFFERENCE WITH THE RATIO X/Z.

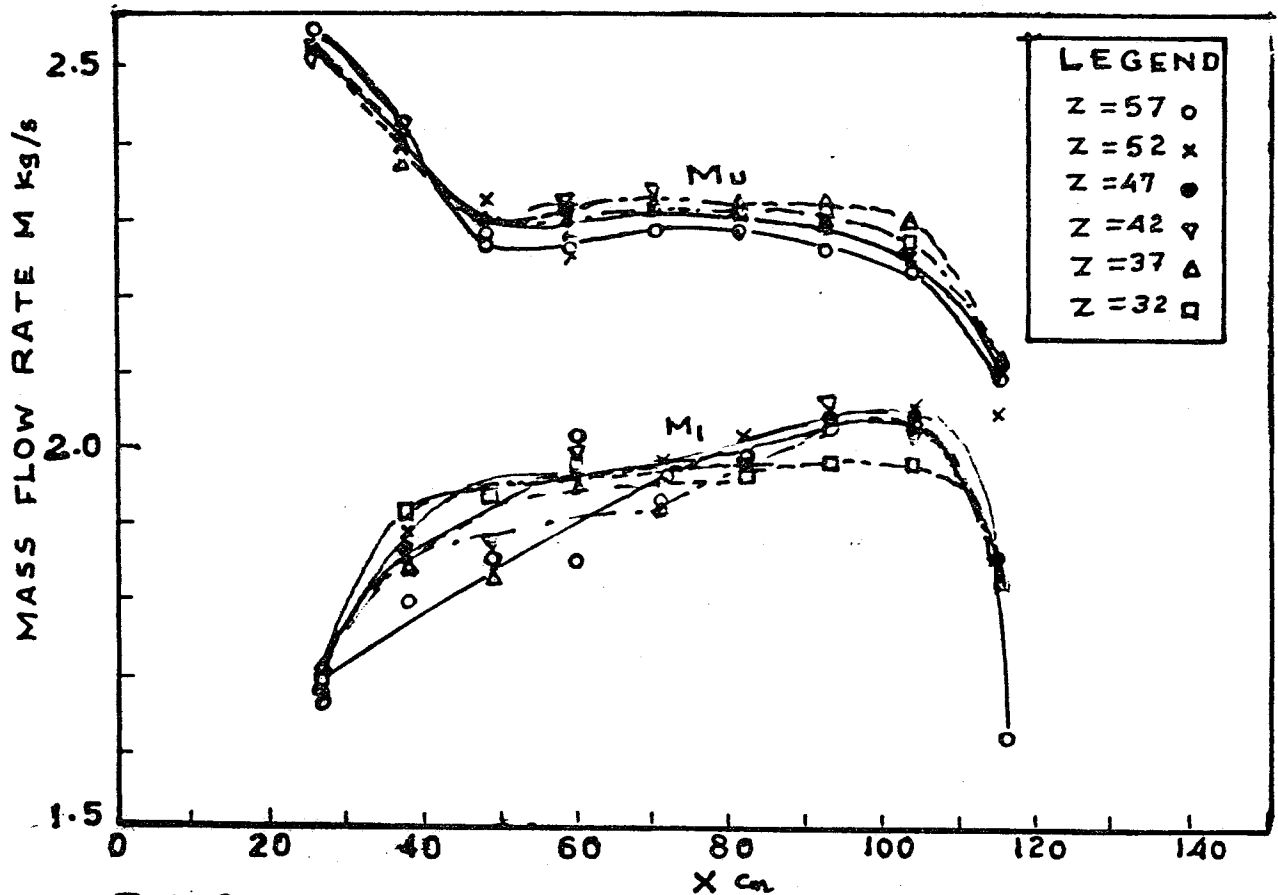


FIG.(8): EFFECT OF X AND Z ON THE MASS FLOW RATE DISTRIBUTION.

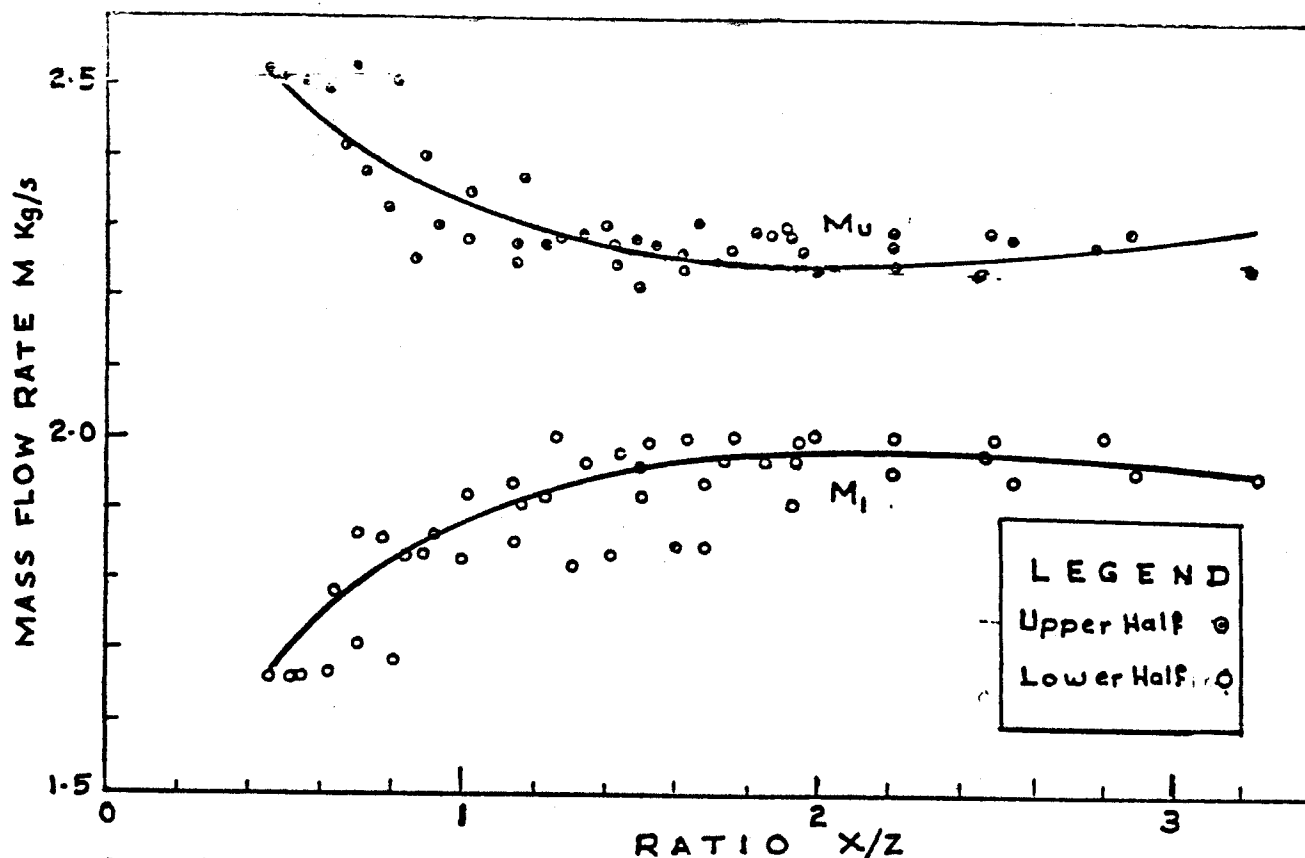


FIG.(9): VARIATION IN MASS FLOW RATE WITH THE RATIO X/Z

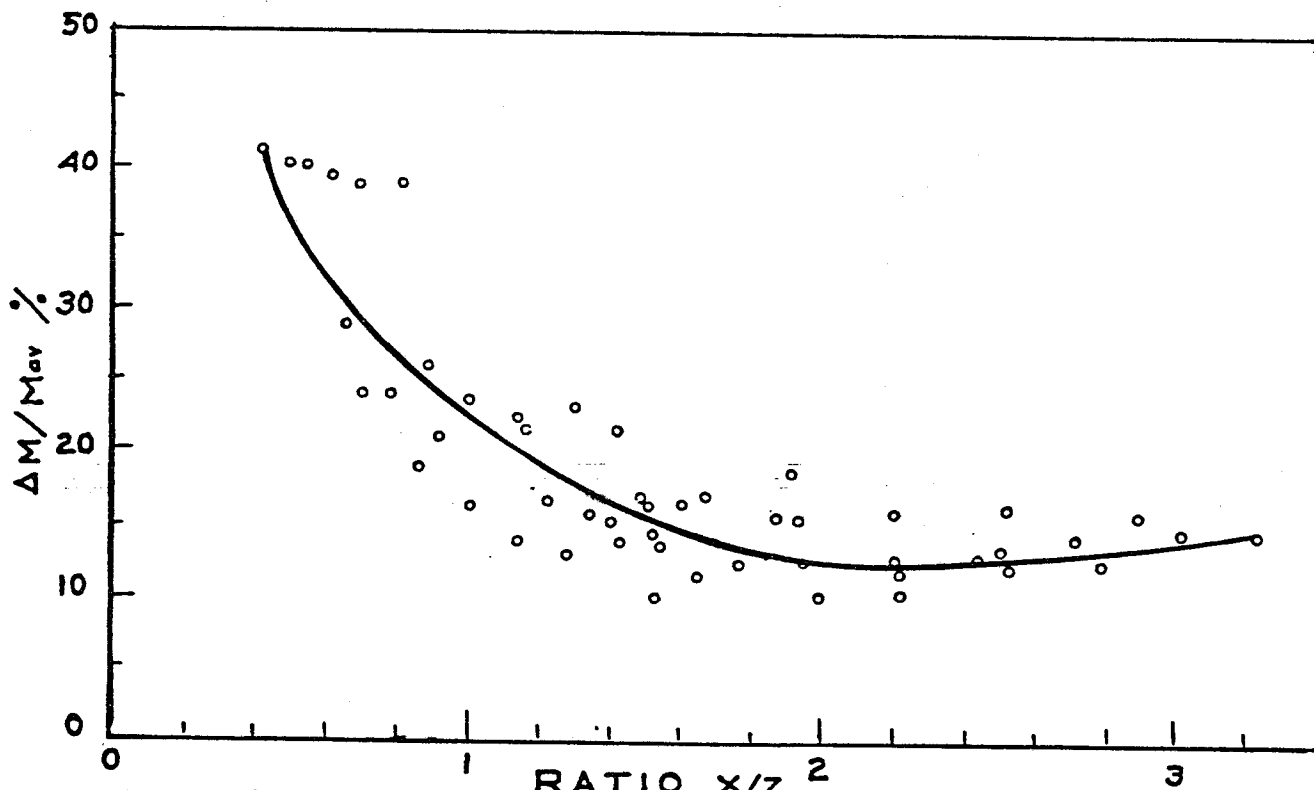
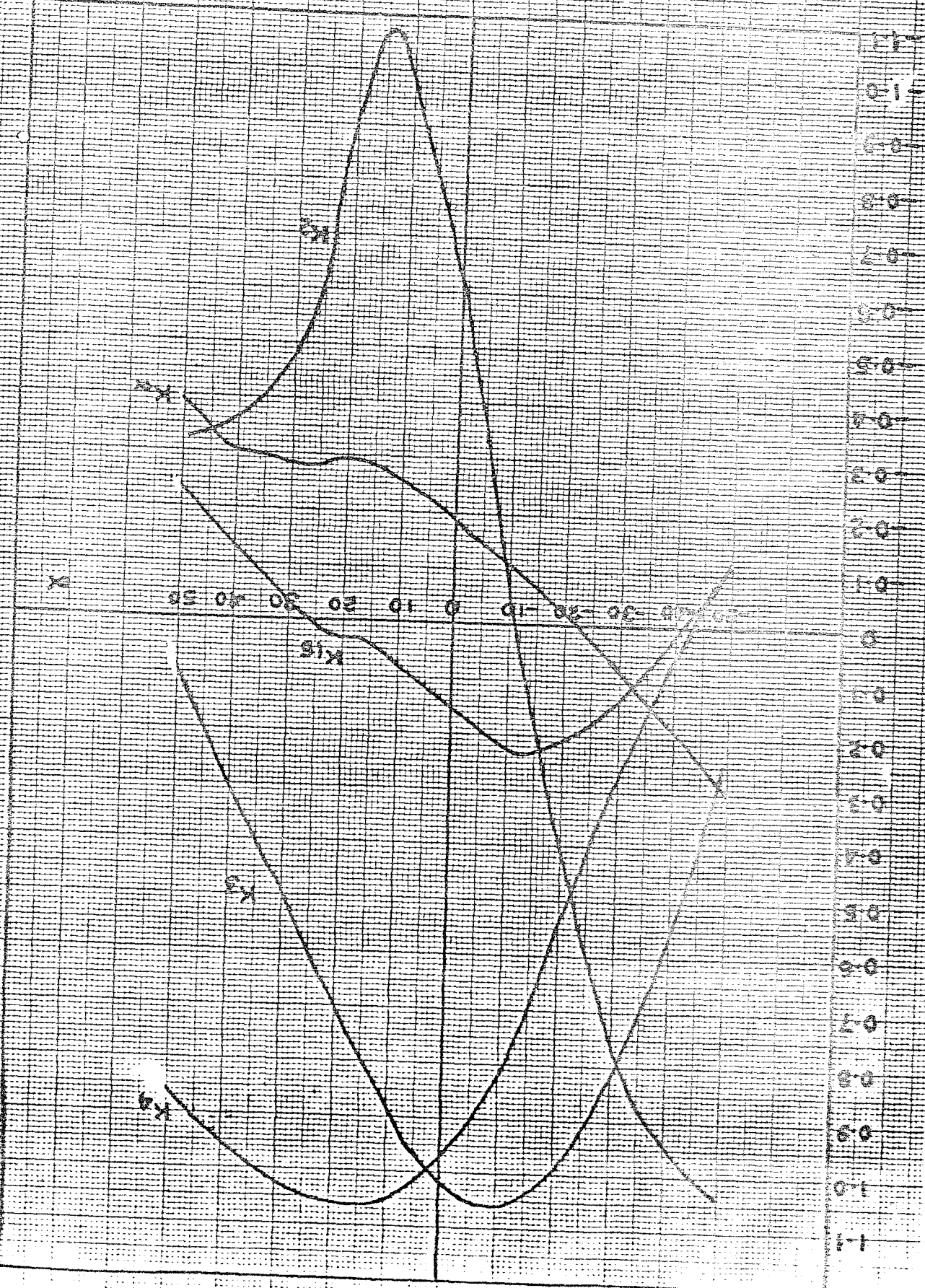


FIG.(10): VARIATION IN PERCENTAGE DIFFERENCE IN MASS FLOW RATE WITH THE RATIO X/Z .

FIGURE 1 CALIBRATION CHART FOR THE CIVIL ENGINEERING PILOT TUBE



APPENDIX B

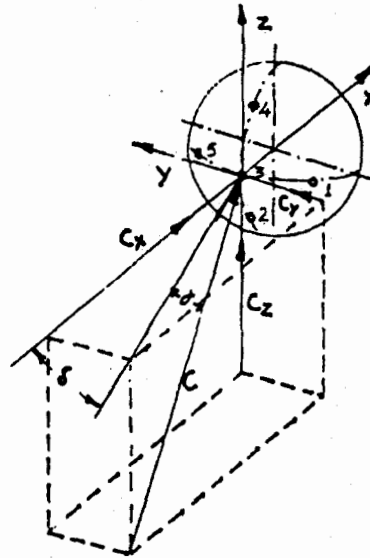


FIG B.2: THE COMPONENTS OF THE VELOCITY IN THE MAIN THREE DIRECTIONS.

```
5 OPEN #1:"LP01"  
10 A$=TIME$  
11 INPUT X  
12 PRINT #1: "N=";X  
13 PRINT #1:" "  
20 INPUT X4,X7  
30 PRINT #1:" X4=";X4;" X7=";X7  
47 PRINT #1:"C", "CX", "CY", "CZ", "P(ST)"  
48 FOR I=1 TO 11  
49 INPUT X1,X2,X3,X5,X6,X8  
50 Q=X1/((X2-X3)*1414.21)  
55 IF(Q<0) THEN Q=-Q  
60 C=X4*(SOR(Q))  
61 X6=(X6*3.14159)/180  
62 X5=(X5*3.14159)/180  
70 CX=C*COS(X6)*COS(X5)  
80 CY=C*COS(X6)*SIN(X5)  
85 CZ=C*SIN(X6)  
90 P=X7+((X8/1414.21)-(X2*Q))  
100 PRINT #1:C,CX,CY,CZ,P  
110 NEXT I  
120 A$=TIME$  
130 PRINT A$,TIME$  
131 PRINT #1:" "  
132 PRINT #1:" "  
133 PRINT #1:" "  
140 END
```

FIG. B3: THE COMPUTER PROGRAM.